$$+ b(b+1)\,\beta^{*2}\,\kappa/R^2\sqrt{\rho_i\mu_i}$$

and

$$\Delta_D = -b(b+1)\beta^{*2}\,\lambda/R^2\sqrt{\rho_i\mu_i} - (b+2)(b-1)\beta^{*2}\,M/R^2\sqrt{\rho_i\mu_i} + 2b(b+2)[(b-1)^2-(b^2-1)]\,M\lambda/R^5\sqrt{\mu_i}\,\rho_i^{3/2}$$

The coefficients in Equation (36) are defined as

$$\alpha_C = -2\sqrt{\mu_o}/R\sqrt{\rho_o} - b(b+2)\epsilon/R^2\sqrt{\rho_o\mu_o} - b(b+2)\kappa/R^2\sqrt{\rho_o\mu_o}$$

$$\gamma_C = [2(2b+1) - 2(b+1)(b+2) - 2b(b+2)]\,\mu_o/\rho_o R^2 - b(b+2)^2\epsilon/\rho_o R^3 + [2(b+2)(b-1) - b^2(b+2)]\,\kappa/\rho_o R^3$$

$$\delta_C = b(b+2)M/R^2\sqrt{\rho_o\mu_o} - 4(b^2-1)(b+2)\mu_o^{3/2}/R^3\rho_o^{3/2} + b(b+2)\lambda/R^2\sqrt{\rho_o\mu_o} + 4(b+2)(2b-1)(b+1)\sqrt{\mu_o}\,\kappa/R^4\,\rho_o^{3/2} - 4b(b+2)(b+1)\,\kappa^2/R^4\,\rho_o^{3/2}\sqrt{\mu_o}$$

$$\xi_C = b(b+2)^2M/R^3\rho_o + \beta^{*2} + 2(2b+1)(b+2)^2b(b+1)\,\mu_o\epsilon/R^5\,\rho_o^2 + 4(b+1)(b+2)(2b+1)(b-1)\mu_o^2/R^4\,\rho_o^2 + [b^2(b+2) - 2(b+2)(b+1)]\,\lambda/R^3\rho_o + 2(b+2)(2b+1)(b^2-2b+2)(b+1)\mu_o\,\kappa/R^5\,\rho_o^2 - 2(2b+1)(b+2)b(b+1)(b+2)\kappa\,\epsilon/R^6\,\rho_o^2 - 2(2b+1)(b+2)b^2(b+1)\,\kappa^2/R^6\,\rho_o^2$$

$$\zeta_C = -2\sqrt{\mu_o}\,\beta^{*2}/R\sqrt{\rho_o} - b(b+2)\epsilon\,\beta^{*2}/R^2\sqrt{\rho_o\mu_o} - 4(b+2)(2b-1)(b+1)\sqrt{\mu_o}\,\lambda/R^4\,\rho_o^{3/2} + 8b(b+2)(b+1)\kappa\,\lambda/R^4\sqrt{\mu_o}\,\rho_o^{3/2} - b(b+2)\beta^{*2}\,\kappa/R^2\sqrt{\rho_o\mu_o}$$

$$\Delta_C = -2b(2b+1)(b+2)^2(b+1)\mu_oM/R^5\rho_o^2 + 2(2b+1)(\mu_o)\beta^{*2}/\rho_o - 2(b+2)(2b+1)(b^2-2b+2)(b+1)\mu_o\lambda/R^5\,\rho_o^2 + 2(2b+1)(b+2)^2(b+1)b\lambda\epsilon/R^6\,\rho_o^2 + 2(2b+1)(b+2)^2(b+1)bM\,\kappa/R^6\,\rho_o^2 + 4(2b+1)(b+2)(b+1)b^2\kappa\lambda/R^6\,\rho_o^2$$

$$\pi_C = b(b+1)(M)\beta^{*2}/R^2\sqrt{\rho_o\mu_o} + b(b+2)\lambda\beta^{*2}/R^2\sqrt{\rho_o\mu_o} - 4b(b+2)(b+1)\lambda^2/R^4\sqrt{\mu_o}\,\rho_o^{3/2}$$

$$\nabla_C = -2(2b+1)(b-2)b(b+1)(b+2)\lambda M/R^6\,\rho_o^2 - 2b^2(b+2)(b+1)(2b+1)\lambda^2/R^6\,\rho_o^2$$

Part II.

Ultra high-speed motion picture photography is used to measure the decay and frequency of drops of liquid in air and of air cavities in liquids. Consequent to the belief that surface active agents induce dynamic interfacial properties, a very clean system is used, and experiments are performed with triple distilled water, tap water, and known aqueous solutions of ionic and nonionic surfactants. Experimental results yield good qualitative agreement with the theory. The theoretical and experimental studies show the system to be a new and promising technique for the quantitative evaluation of the various interfacial viscous and elastic properties.

The main objective of the experiment was to accurately measure the decay and frequency characteristics of dispersed phases oscillating in a continuous medium under controlled conditions. The controls that had to be exercised were on the size of the drop or bubble and the characteristics of the interface, namely, the amount of surface active material that is present on it.

The basic requirement of the experimental setup was that an oscillating dispersed phase, once released by suitable means in a continuous medium, could be examined and its behavior recorded. Since the effect of surfactants had also to be studied, the system had to be clean. The equipment was built along the lines outlined by Loshak (1969), and Loshak and Byers (1973). The overall requirements to be met by the apparatus can be listed as follows.

A transparent section woud be needed which would permit visual observation of the motion of the dispersed phase. Plane sheet glass was used for the front and back, while the sides were constructed of aluminum. Provision for controlled and measurable formation and injection of the dispersed phase into the continuous medium would be required. An oscillating mechanism had to be provided to make the dispersed phase oscillate at any desired frequency. A high speed motion picture camera system along with frame by frame analysis facilities would be needed to record rapid decay and frequencies of the oscillations. A choice of surfactants with which the dynamic interfacial properties could be altered had to be provided.

THE EXPERIMENTAL SETUP

The test section was rectangular in cross section, made of aluminum at the sides, and plane sheet glass for the front and back to minimize optical distortion. It was about 19 in. long. Larger square cross-sectional containers at the top and bottom were provided to collect the dispersed phase. Injection mechanisms were provided at three points along the sides of the column, two very near the top and one near the bottom. This would enable us to study both rising and falling media.

The injection mechanism consisted of a tip made out of concentric copper tubes. The end of the tip was a detachable syringe needle made of high quality chromium steels. All sizes ranging from BD18 to BD27 were used. The number refers to the size of the needle; the larger it is the smaller the diameter. A BD22 needle would approximately be about 0.0286 in. diameter and about 3.5 in. long. The needle was bent through 90 deg so that the

drop or bubble could be released from a vertical position. In the case of the drop in air, it was obviously bent downward, while in the case of the bubble in water, it was bent upwards. The remainder of the injection mechanism consisted of an outer tubing of about 16 gauge, through which the fluid actually passed. One end of the narrow tubing was connected to the syringe needle, while the other end was connected to a Luer attachment to which a syringe could be fitted. The type of syringe used was a Microburet syringe controlled by a syringe microburet model No. SB2 manufactured by the Micro-metric Instrument Company, Cleveland, Ohio. This syringe was calibrated at 0.2 μl per division. The injection mechanism was inserted through the holes provided on the sides of the test section and was held in place by a bracket mounted on the outside.

The oscillation in the dispersed medium was initiated by using an electromechanical shaker (Calydene model 6C). It was mounted on the side of the test section in contact with the injection mechanism. The vibrator frequency was controlled by an audio amplifier and frequency generator. An accurate measure of the decay and frequency was made with a high speed motion picture camera, Hycam model (100 ft type) No. K20SIR. This camera was capable of speeds up to 10 000 frames/s. The actual speed used depended on the frequency to be studied, and a rough estimate of that could be obtained from the theoretical calculations. The camera was capable of taking in 100 ft rolls at a time. The speed of the camera was controlled by a variac which could vary the speed continuously from 100 to 10 000. A Milli-mite model No. TLG-3, timing light generator made by the Red Lake Labs, was connected to the camera. This made light marks on the film at every 1/1 000th of a second and enabled one to measure the speed accurately. To enable a closer study of the dispersed phase, a 135 mm Soligor Telephoto lens with a set of Miranda close-up lenses were used. In this way, a reasonably large image of the drop could be observed. In order to achieve proper exposures with such high speeds being involved, a set of DXC Photo flood, 500 w lamps were used. The number of these depended on the speed at which the camera was used. Normally, at least four of them were used. Since flood lamps cause spots on the film, the light had to be diffused through a diffuser, which was interposed between the lamps and the column. The resulting pictures of the dispersed phase oscillations were analyzed by using a Lafayette Instrument Co., Analyst Model No. AAP-K, 16 mm movie projector. This projector had facilities for single frame, slow motion, and reverse action, all of which were required to make the analysis of the films possible.

Two types of surfactants were used, one of the ionic type and one of the nonionic type. Both were soluble in water. The criteria for their selection are detailed elsewhere (Ramabhadran, 1972).

EXPERIMENTAL PROCEDURE

One of the foremost considerations of the experiment was cleanliness of the system. The whole system was washed thoroughly with tap water and then with distilled water a number of times. Distilled water was always used as the solvent for both the drop and the cavity experiment. The supply distilled water was carefully distilled again by using a Barnstead still and sterilizer (model No. 2816064). Solutions of accurately known concentrations of surface active agents were prepared. The method of preparation depended on whether it was the drop or the cavity experiment. After the liquid phase was carefully prepared, the injection mechanism was thoroughly cleaned and filled with the dispersed phase. At this point the high

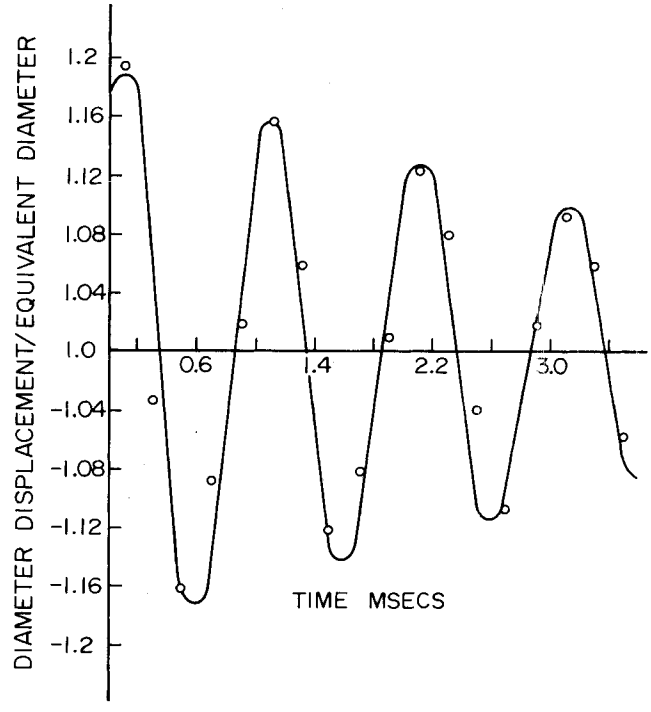

Fig. 1. Typical oscillation curve.

speed motion picture camera arrangement was set up and focused as accurately as possible. Tri-X reversal, TXR-7278, type 430 motion picture film, ASA 160, was used. The entire column was now filled with the continuous medium. The power amplifier and the low frequency oscillator were switched on, and the proper frequencies and amplitudes were selected. The proper frequency was arrived at by using the theoretical values as approximate guidelines and by trial and error, and usually very low amplitudes were used. The oscillator system imparted to the syringe tip the desired frequency.

The timing light generator was now turned on and allowed to warm up. The variac was connected to the camera to control its speed, and the desired voltage was set in it. Now the flood lighting system was turned on. A slow stream of the dispersed phase was allowed to form at the end of the injection mechanism. When the dispersed phase reached a certain size, it detached itself from the oscillating tip. This size depended on the applied frequency of oscillation and the physical characteristics of the dispersed phase. After leaving the tip, they would oscillate and decay and finally fall through the continuous phase as an almost spherical drop. To ensure that aging is complete, the dispersed phase was formed as slowly as possible. As the dispersed phase left the tip, the camera was turned on and thus the motion recorded.

With the analyst projector used, each film was carefully examined and a frame count made between each oscillation. Also, at each extreme, the dimensions of the drop were measured as accurately as possible. By knowing the time between oscillations, the frequency could be obtained. The extreme points of the oscillation were plotted logarithmically against time, the slope of which gives the decay rate. Thus, for each run the two desired pieces of information can be obtained, namely, the decay factor and frequency.

No specific difficulties were encountered with the drop experiment. Camera speeds between 7 000 and 10 000 frames/s were used, and the best data were obtained for drop diameters between 0.9 and 1.1 mm. However, for the same size range, the frequency of the cavities were much higher. Consequently, camera speeds restricted the diameter range to 0.9 mm or higher. In both cases the

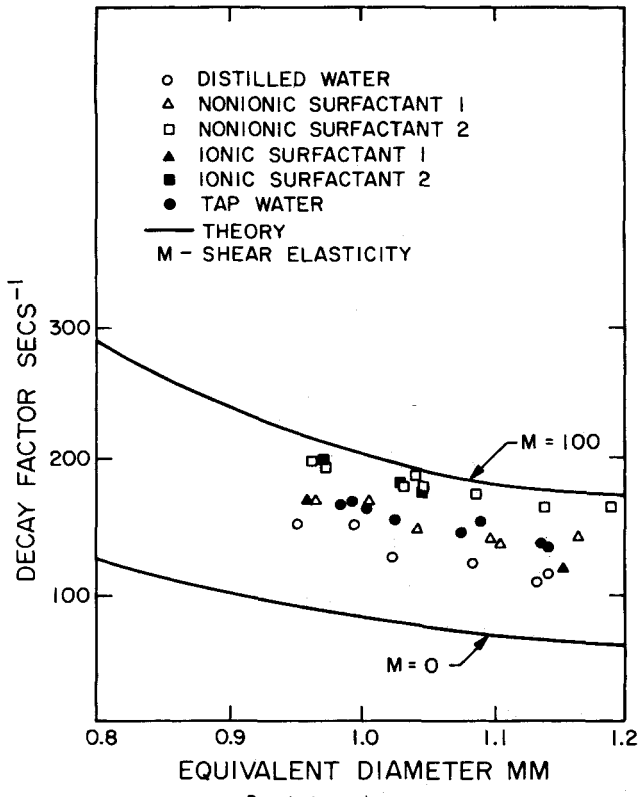

Fig. 2. Drop data.

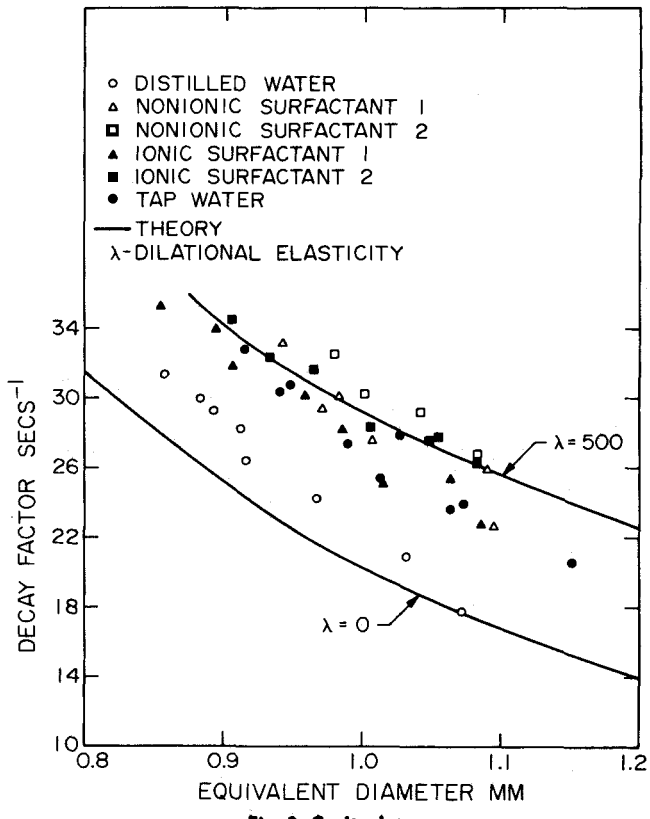

Fig. 3. Cavity data.

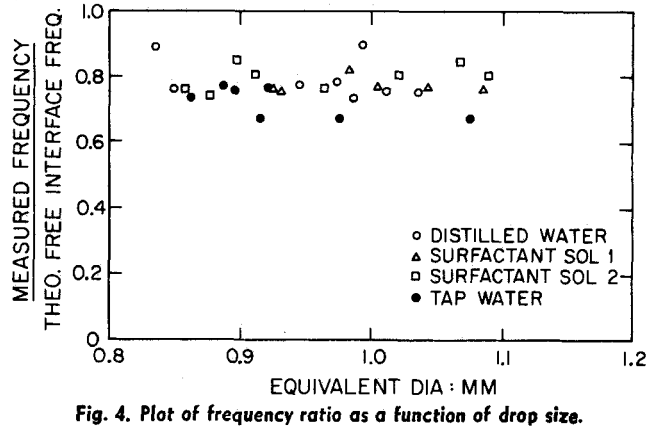

Fig. 4. Plot of frequency ratio as a function of drop size.

resolution of the lenses used was very good, and excellent photographs of the prolate-oblate oscillations were obtained.

RESULTS

The experiments were performed for pure distilled water, two solutions of different concentrations of each of the surfactants, and ordinary tap water. The same experiments were repeated for the drop and the cavity. For each liquid, different diameters of the dispersed phase were studied. The films were analyzed frame by frame, and a typical oscillation curve for a drop is shown in Figure 1. The logarithm of the peak heights were then plotted against time to obtain the decay factor. In Figure 2 the measured decay of drops is plotted against equivalent diameter. The theoretical curves from Figure 1 of Part II are also superimposed. It is fairly clear that the decay factors change with surfactant concentration in the same direction as increasing dilational elasticity. The curve for $\lambda = 0$ corresponds to that of a free interface. The measured frequencies were consistent with the expected values given the interfacial tension, indicating that the rheological character of the interface does not seem to influence it. This is in line with the theoretical conclusions on the frequency. Figure 3 shows the frequency data for drops. In Figure 4 the measured decay of bubbles is plotted against equivalent diameters together with the theoretical curves from Figure 4 of Part I. Once again, it is clear that the decay factors change with surfactant concentration in the same direction as increasing shear elasticity. The frequencies exhibited the same behavior as that in the drop study.

DISCUSSION OF THE THEORY AND EXPERIMENT

From a point of view of the study of interfacial mechanics, the most important variables in the problem are the decay and the frequency of oscillation of the dispersed phases. In the range of drop and cavity diameters considered, the most important parameter seems to be the interfacial elasticities. Numerical calculations do seem to indicate that in the case of the drop the dominant effect is due to the interfacial dilational elasticity which functions as a stabilizing force. Physically, an increasing dilation would imply that the surface of the drop behaves more and more like a solid and at very large dilation essentially becomes inextensible. A free interface corresponds to one whose surface properties are all nonexistent. The data with very pure distilled water also seem to deviate from calculations based on a free interface. This indicates that surfactant free interfaces also have some intrinsic rheological character and that a free interface corresponds to an ideal fluid, inelastic and inviscid. Addition of surface active material alters the nature of the interface; its interfacial tension is lowered and presumably dynamic interfacial properties are introduced due to gradients in interfacial tension. The numerical calculations with the cavity indicate that the dominant effect is due to interfacial shear elasticity. Once again, data with very pure distilled water deviate from the free interface calculations, indicating the possible existence of intrinsic rheological properties in the

interface. Furthermore, in both the drop and the cavity experiment, the experimental data follow the same trend as the theory, which is very encouraging. It might be noted that in both the analysis and the experiment the effect of the dynamic properties on the frequencies was insignificant. Addition of surfactants lowered the frequency, but this was entirely commensurate with the lower interfacial tension.

The main conclusion drawn from this analysis and experiment is that working with different systems (gas-liquid, liquid-liquid, liquid-gas) in different size ranges, all the interfacial properties can presumably be backed out for a given surfactant or even a pure fluid. The significance (or the lack) of these properties can therefore be estimated. A large number of such similar experiments needs to be done before final conclusions can be made.

LITERATURE CITED

Leshak, J., "Forced Oscillations of Drops in a Viscous Medium," M.S. thesis, Univ. Rochester, New York (1969).

———, and C. H. Byers, "Forced Oscillations of Drops in a Viscous Medium," *Chem. Eng. Sci.*, 28, 149 (1973).

Ramabhadran, T. E., "Inference of Dynamic Interfacial Properties from an Oscillating Drop and Bubble," Ph.D. thesis, Univ. Rochester, New York (1972).

Manuscript received September 19, 1975; revision received May 17, and accepted May 18, 1976.

Diffusion of Hydrocarbons in 13X Zeolite

The kinetics of sorption of four representative hydrocarbons in 13X zeolite crystals have been investigated at temperatures within the range 409 to 513°K and pressures 0.1 to 100 torr. Extensive diffusivity data are presented showing the dependence on sorbate concentration and temperature. The form of the concentration dependence of the diffusivity for these systems is very similar to that of the small monatomic and diatomic molecules in 5A zeolite. This similarity is understandable, since the key factor which determines the diffusion behavior is the relative size of diffusing molecule and sieve window. For these hydrocarbons in the 13X sieve, as for the monatomic and diatomic gases in 5A, the critical diameters of the diffusing molecules are all appreciably smaller than the free diameter of the windows.

DOUGLAS M. RUTHVEN
and
INGO H. DOETSCH

Department of Chemical Engineering
University of New Brunswick
Fredericton, N.B., Canada

SCOPE

Despite the widespread application of the X and Y zeolites as cracking catalysts, available information on the diffusion of hydrocarbons in these materials is sparse. This is because the crystal size of the commercially available X and Y zeolites is small ($\sim 1\mu m$), and the diffusional time constants are therefore too small to be determined by conventional techniques. In the present study, a specially prepared sample of 13X zeolite with crystal size $\sim 16.5\mu m$ was used in order to achieve sorption rates which were slow enough to measure gravimetrically. Diffusivities were determined for four representative hydrocarbons (nC_7H_{16}, C_6H_{12}, C_6H_6, and $C_6H_5 \cdot CH_3$) over a range of temperatures from 409° to 513°K and pressures 0.1 to 100 torr. The concentration and temperature dependence of the diffusivity have been studied in detail, and comparative data for the diffusion of nC_7H_{16} in 5A zeolite are presented for a similar range of pressure and temperature.

CONCLUSIONS AND SIGNIFICANCE

Diffusivities for the four hydrocarbons in 13X zeolite are strongly concentration dependent, and the pattern of concentration dependence is similar to that observed previously for the diffusion of small monatomic and diatomic molecules in 5A zeolite (Ruthven and Derrah, 1975) and distinctly different from the behavior of the light hydrocarbons in the A zeolite (Ruthven, Loughlin, and Derrah, 1973). Over the range of the experimental measurements, the diffusivities for the C_6 and C_7 species in 13X sieve are of order $10^{-8} - 10^{-9}$ $cm^2 \cdot s^{-1}$, which is more than an order of magnitude greater than the diffusivities for *n*-heptane in 5A sieve under comparable conditions. The diffusional activation energies for the C_6 and C_7 hydrocarbons in 13X sieve range from 5.0 to 6.2 kcal, and there is no correlation with critical molecular diameter. By contrast, activation energies for the light hydrocarbons in the 5A sieve show a clear correlation with molecular diameter and a different pattern of concentration dependence of diffusivity. The key factor which determines the diffusional behavior is the relative size of the diffusing molecule and the sieve window. On this basis, the similarities of the present systems with the behavior of small monatomic and diatomic molecules in the 5A sieve and the pronounced differences from the behavior of the hydrocarbons in 5A sieve are clearly understandable.